Electronic Supplementary Material (ESI) for Inorganic Chemistry Frontiers.

Electronic Supplementary Material

Pushing Capacities and Energy Densities Beyond Theoretical Limits of Lithium Primary Batteries using active CFx Nanocapsules with x > 1

Yifan Liu[a,b], Hongyan Zhang[a,b], Baoshan Wu[a,b], Jianyi Ma[c], Guoyun Zhou[a,*], Nasir Mahmood[d,*], Xian Jian[a,b,*] , Huakun Liu[e]

[a]School of Materials and Energy, University of Electronic Science and Technology of China, Chengdu, 611731, China.
[b]Yangtze Delta Region Institute (Huzhou), University of Electronic Science and Technology of China, Huzhou 313001, China.
[c]Institute of Atomic and Molecular Physics, Sichuan University, Chengdu, 610065, China.
[d]School of Engineering, RMIT University, VIC 3001 Australia.
[e]Institute for Superconducting and Electronic Materials, University of Wollongong, Wollongong, NSW 2522, Australia.

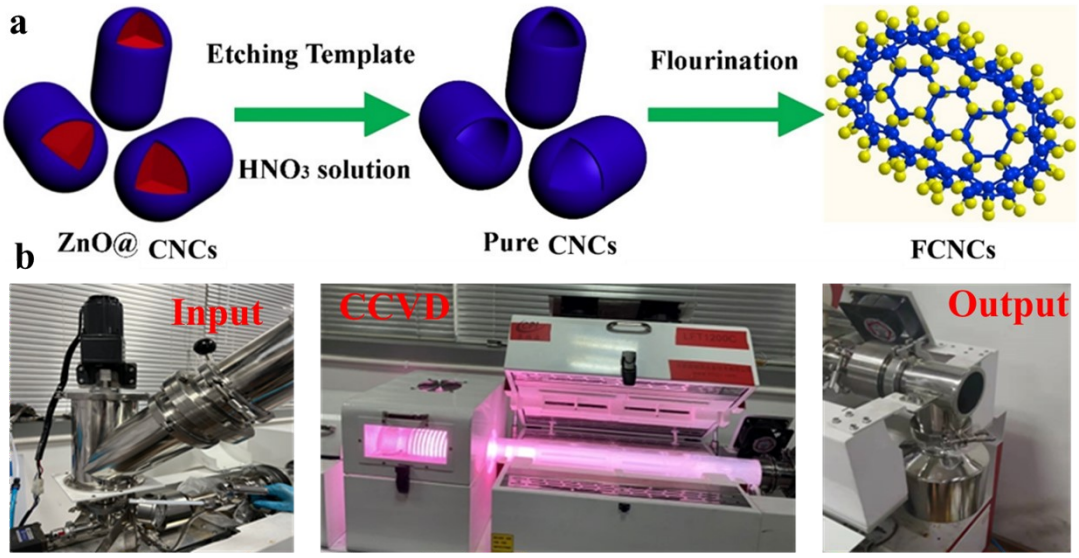

Figure S1. a. Schematic diagram of the synthetic route of CFNCs. b. The lab-made serialized CCVD device to prepare CNCs.

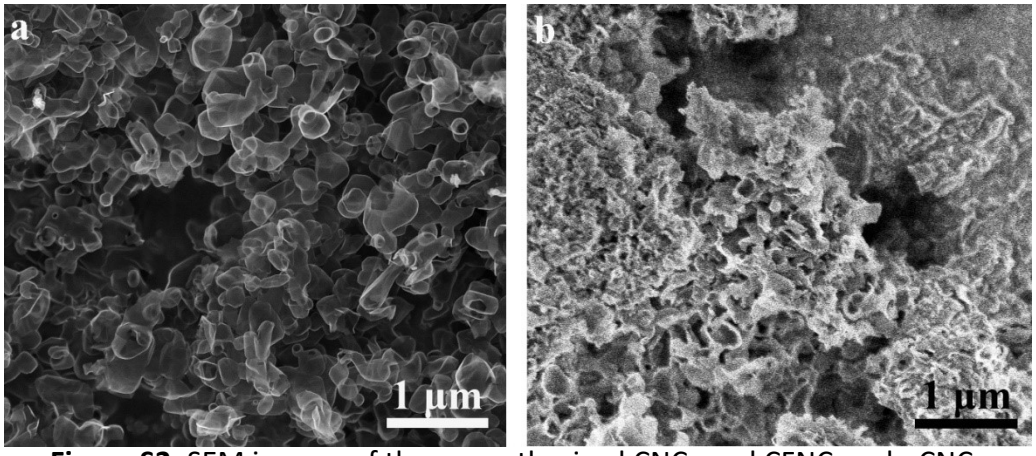

Figure S2. SEM images of the as-synthesized CNCs and CFNCs. a-b, CNCs synthesized by CCVD method. c-d, CFNCs–360 synthesized by fluorination process (without gold coating before recording SEM).

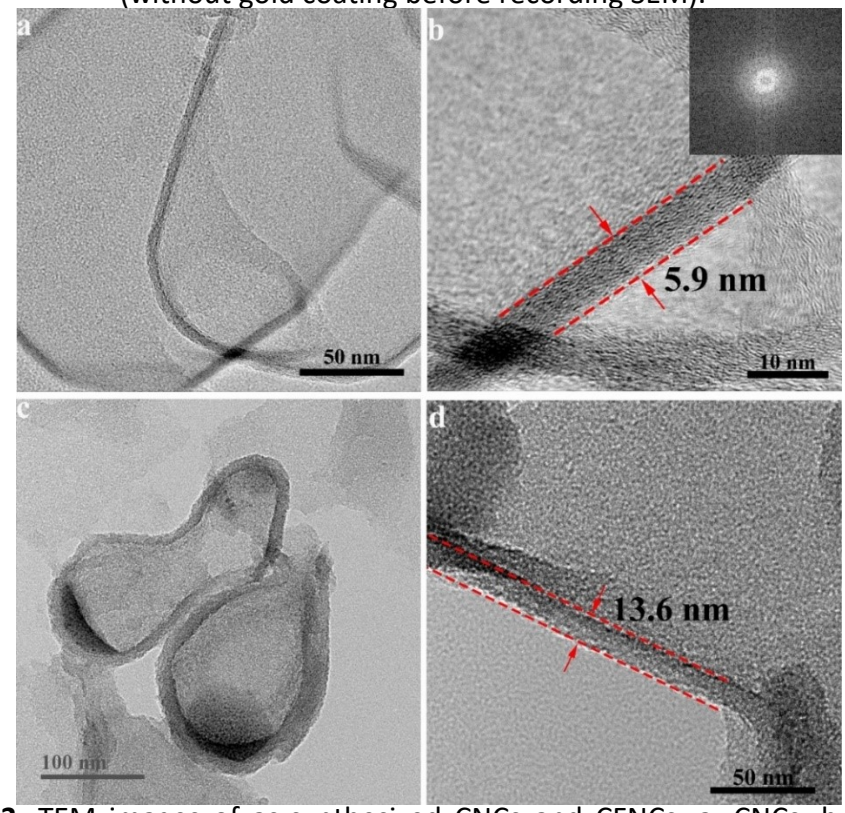

Figure S3. TEM images of as-synthesized CNCs and CFNCs. a, CNCs. b, the wall thickness of 5.9 nm for CNCs. c, CFNCs. d, the wall thickness of 13.6 nm for CFNCs.

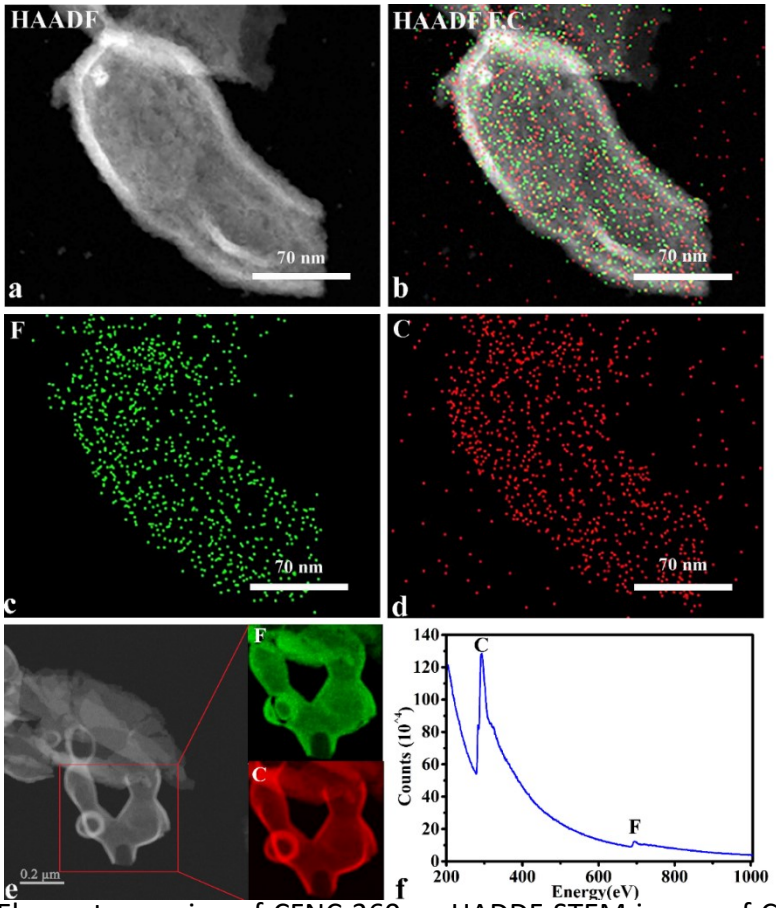

Figure S4. Element mapping of CFNC-360. a, HADDF-STEM image of CFNC-360. b, the distribution of F, C elements on the CFNC-360. c, F element. d, C element. e, EELS mapping for the selected zone. f, the EELS spectrum of the selected zone.

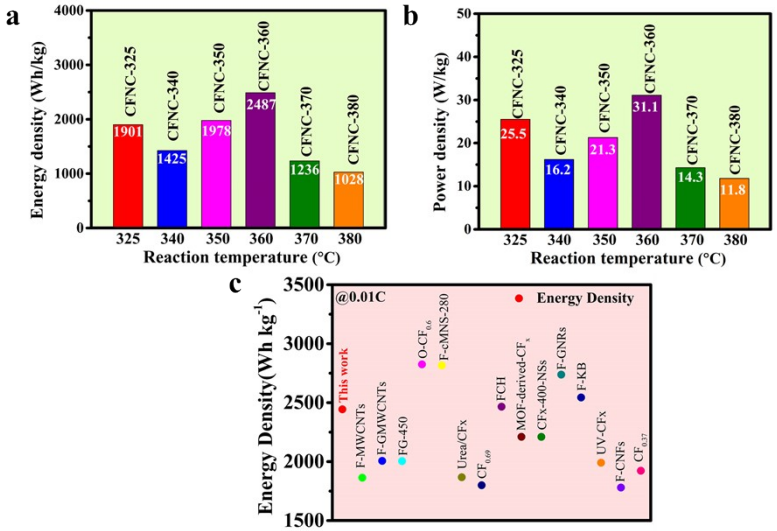

Figure S5. a, the energy density of CFNCs synthesized at different temperatures for Li/CFx battery. b, the power density of CFNCs synthesized at different temperatures for Li/CFx battery. c. comparison of energy density for CFNC-360 with various art exemplar fluorinated carbon active materials.

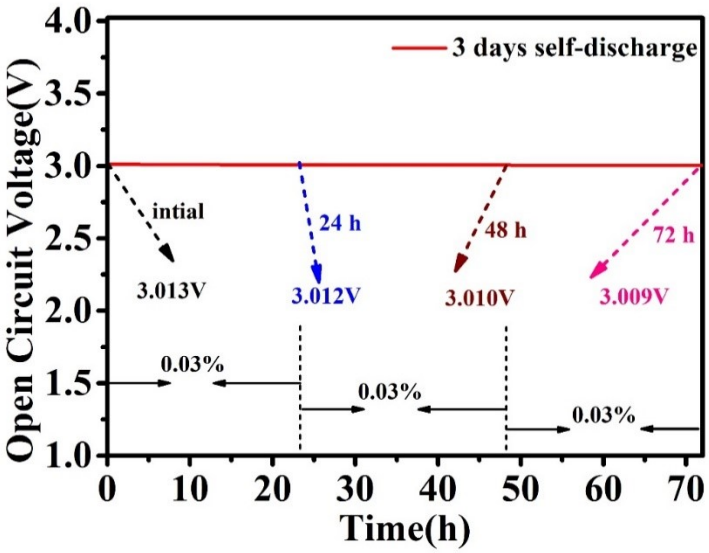

Figure S6. OCV stability of Li/CFx primary battery loaded with CFNCs materials testing over 3 days period.

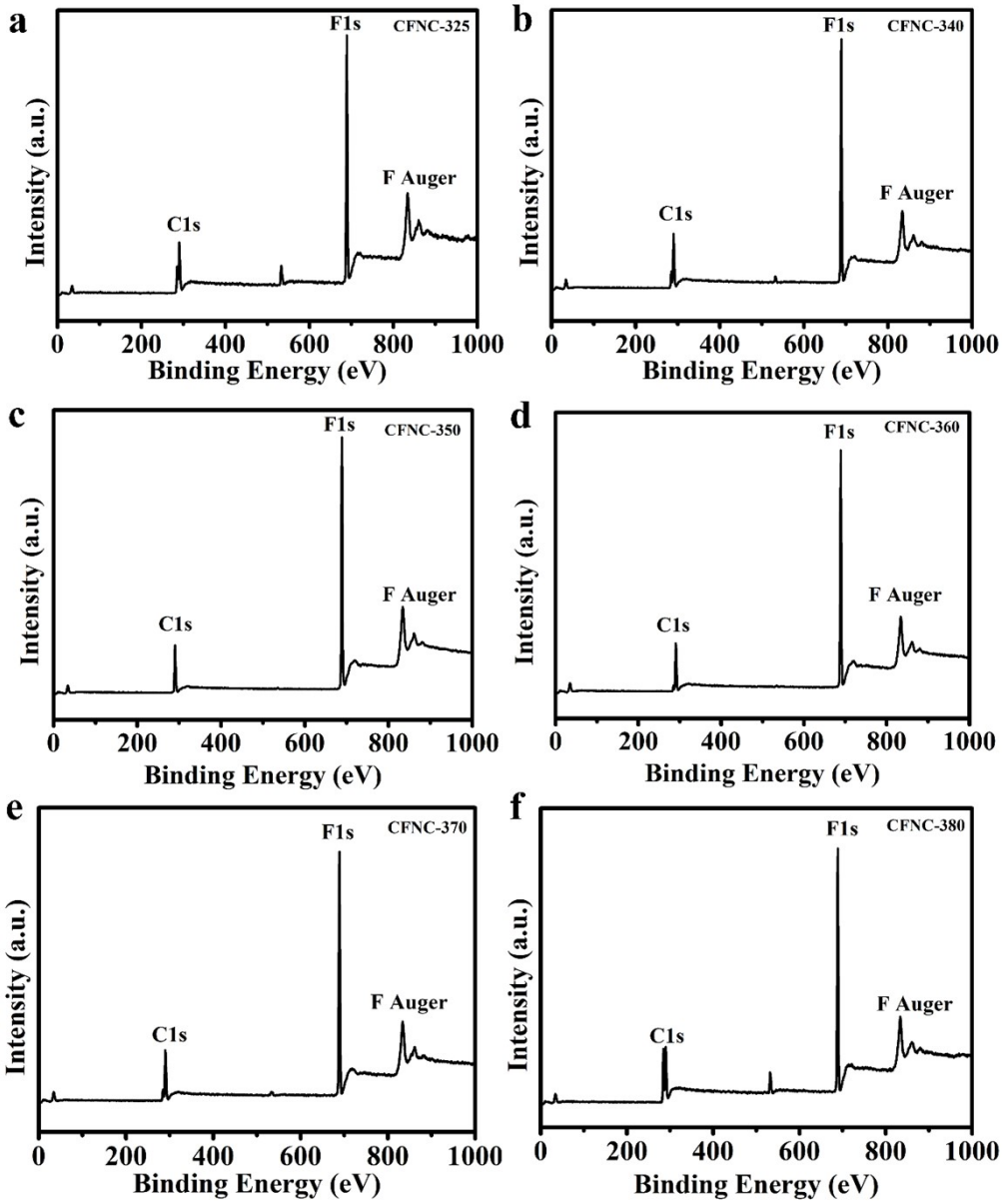

Figure S7. Survey spectrum of CFNCs. a, CFNC–325. b, CFNC–340. c, CFNC–350. d, CFNC–360. e, CFNC–370. f, CFNC–380.

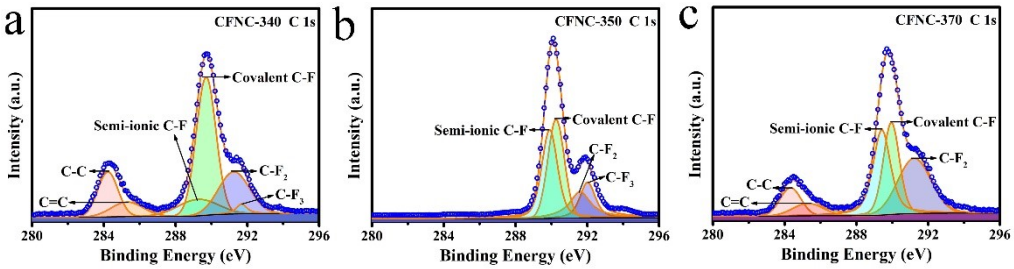

Figure S8. High-resolution XPS spectra of C1s for as-synthesized CFNCs prepared under different reaction temperatures. (a), 340℃. (b) 350℃. (c) 370℃.

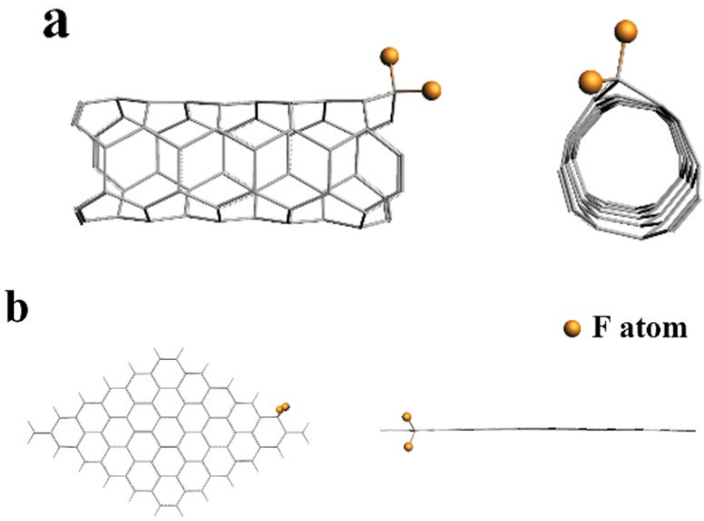

Figure S9. Schematic diagram of the fluorinated carbon materials with different curvatures from different viewing angles. (a) C-F_2 bond binding on carbon nanotubes with a radius of 2.15 Å, and (b) C-F_2 bond binding on graphene fragments with an infinite radius.

Table S1. The total transition metal (Fe, Co and Ni) content of CFNC–360 detected by ICP-AES.

Sample	Fe (wt.%)	Co (wt.%)	Ni (wt.%)	Zn (wt.%)
CFNC–360	0.0028	<0.0001	<0.0001	<0.0001

Table S2. Galvanostatic discharge performance of CFNCs at a discharge rate of 0.01C.

Samples	CFNC–325	CFNC–340	CFNC 350	CFNC–360	CFNC–370	CFNC–380
F/C ratio	0.97	1.17	1.49	1.61	1.51	1.37
Q_{theo} (mAh g^{-1})	854	916	991	1013	995	966
Q_{exp} (mAh g^{-1})	735	554	789	1056	502	429
Energy density (Wh kg^{-1})	1901	1425	1978	2487	1236	1028

Table S3. The fitting parameters of Electrochemical impedance spectroscopy (EIS) for CFNCs.

Samples	CFNC-325	CFNC-340	CFNC -350	CFNC -360
R_s (Ω)	5.8	4.7	4.6	4.8
R_{ct} (Ω)	157	433	718	148
Z_w ($S^{1/2}$)	$1.6e^{-3}$	$1.23e^{-3}$	$6.44e^{-4}$	$4.5e^{-3}$

Table S4. Comparison of the performance CFNC-360 with the reported literature for specific capacity and energy density at 0.01C (1C=821mA g^{-1}).

Nominal materials	**Discharge Capacity (mAh g^{-1})**	**Energy Density (Wh kg^{-1})**	**Discharge rate (C-rate)**	**Reference**
CFNC-360	1056	2487	0.01C	This work
Fluorinated multi-walled carbon nanotubes (FCNTs)	764.0	1863.9	0.01C	S[1]
Fluorinated graphitized multiwalled carbon nanotubes (FGCNTs)	798.8	2006.6	0.01C	S[1]
Fluorinated Nanographite (FG-450)	837.4	2004.5	0.01C	S[2]
Oxidized sub-fluorinated graphite Fluorides (O-$CF_{0.6}$)	870	2825	0.01C	S[3]
fluorinated calcinated macadamia nut shell (F-cMNS-280)	949	2816	0.01C	S[3]
Urea-assistant ball-milled CFx (Urea/CFx)	747.3	1867.9	0.01C	S[4]
$CF_{0.69}$	647	1880	0.01C	S[5]
fluorinated hard carbon (FHC)	922.6	2466	0.01C	S[6]
MOF-derived nano-porous fluorinated carbon (MOF-derived-CFx)	850.3	2110.7	0.01C	S[7]
Fluorinated graphite nanosheets (CFx-400 NSs)	921	2210	0.01C	S[8]
Fluorinated graphene nanoribbons (F-GNRs)	939.2	2738	0.01C	S[9]
fluorinated ketjenblack (FKB)	924.6	2544	0.01C	S[10]
UV-radiation fluorinated carbon (UV-CFx)	798.2	1990.9	0.01C	S[11]
fluorinated Carbon nanofibers (FCNFs)	748	1780	0.01C	S[12]
Sub-fluorinated thin carbon nanotubes ($CF_{0.37}$)	900	1923	0.01C	S[13]

Table S5. Surface chemical bond contents for various CFNCs based on XPS analysis.

Sample	Different bonds content (at%)

	C-C	C=C	Semi-ionic C-F	Covalent C-F	$C-F_2$	$C-F_3$
FGC-325	21.0	14.3	11.2	34.1	9.9	9.5
FGC-340	14.6	7.5	10.6	44.0	21.0	2.3
FGC-350	-	-	34.4	34.5	17.3	13.8
FGC-360	7.3	-	33.6	37.2	15.1	6.8
FGC-370	9.4	6.1	29.9	25.5	29.2	-
FGC-380	41.7	7.2	3.4	36.4	11.3	-

Table S6. F/C ratios for various CFNCs based on XPS observations.

Samples	CFNC–325	CFNC –340	CFNC 350	CFNC –360	CFNC –370	CFNC –380
F/C ratio	0.92	1.07	1.47	1.24	1.15	0.71

Table S7. Binding energies of $C_{24}F_{36}Li$ supercell structure in air and aqueous systems.

Structure	E1(eV)	E2(eV)	ΔE(eV)
$C_{24}F_{36}Li$-g	0.79	0.67	0.12
$C_{24}F_{36}Li$-s	2.36	0.74	1.62

Table S8. Bonding energies of $C-F_2$ with different curvatures.

Model	$C_{tube}-F_2$	$C_{plane}-F_2$
$E_{\text{bonding energy}}$ (Kcal/mol)	105.81	143.66

References

1. Y. Y. Li, X. Z. Wu, C. Liu, S. Wang, P. F. Zhou, T. Zhou, Z. C. Miao, W. Xing, S. P. Zhuo and J. Zhou, Fluorinated multi-walled carbon nanotubes as cathode materials of lithium and sodium primary batteries: effect of graphitization of carbon nanotubes, *J Mater Chem A*, 2019, **7**, 7128-7137.
2. L. Wang, Y. Y. Li, S. Wang, P. F. Zhou, Z. D. Zhao, X. W. Li, J. Zhou and S. P. Zhuo, Fluorinated Nanographite as a Cathode Material for Lithium Primary Batteries, *Chemelectrochem*, 2019, **6**, 2201-2207.
3. M. Mar, M. Dubois, K. Guerin, N. Batisse, B. Simon and P. Bernard, High energy primary lithium battery using oxidized sub-fluorinated graphite fluorides, *Journal of Fluorine Chemistry*, 2019, **227**.
4. P. Zhou, J. Weng, X. Liu, Y. Li, L. Wang, X. Wu, T. Zhou, J. Zhou and S. Zhuo, Urea-assistant ball-milled CFx as electrode material for primary lithium battery with improved energy density and power density, *J. Power Sources*, 2019, **414**, 210-217.
5. Q. Zhang, K. J. Takeuchi, E. S. Takeuchi and A. C. Marschilok, Progress towards high-power Li/CFx batteries: electrode architectures using carbon nanotubes with CFx, *Physical Chemistry Chemical Physics*, 2015, **17**, 22504-22518.
6. R. X. Zhou, Y. Li, Y. Y. Feng, C. Peng and W. Feng, The electrochemical performances of fluorinated hard carbon as the cathode of lithium primary batteries, *Composites Communications*, 2020, **21**.
7. X. T. Li, H. C. Zhang, C. Liu, J. Y. Qiao and X. M. Zhou, A MOF-derived multifunctional nano-porous fluorinated carbon for high performance lithium/fluorinated carbon primary batteries, *Micropor Mesopor*

Mat, 2021, **310**.

8. X. X. Yang, G. J. Zhang, B. S. Bai, Y. Li, Y. X. Li, Y. Yang, X. Jian and X. W. Wang, Fluorinated graphite nanosheets for ultrahigh-capacity lithium primary batteries, *Rare Metals*, 2021, **40**, 1708-1718.
9. C. Peng, L. C. Kong, Y. Li, H. Y. Fu, L. D. Sun, Y. Y. Feng and W. Feng, Fluorinated graphene nanoribbons from unzipped single-walled carbon nanotubes for ultrahigh energy density lithium-fluorinated carbon batteries, *Science China-Materials*, 2021, **64**, 1367-1377.
10. S. B. Jiang, P. Huang, J. C. Lu and Z. C. Liu, The electrochemical performance of fluorinated ketjenblack as a cathode for lithium/fluorinated carbon batteries, *Rsc Advances*, 2021, **11**, 25461-25470.
11. J. Ma, Y. F. Liu, Y. Peng, X. X. Yang, J. Hou, C. Liu, Z. W. Fang and X. Jian, UV-radiation inducing strategy to tune fluorinated carbon bonds delivering the high-rate Li/CFx primary batteries, *Compos Part B-Eng*, 2022, **230**.
12. Y. Ahmad, K. Guérin, M. Dubois, W. Zhang and A. Hamwi, Enhanced performances in primary lithium batteries of fluorinated carbon nanofibers through static fluorination, *Electrochim. Acta*, 2013, **114**, 142-151.
13. Y. Ahmad, M. Dubois, K. Guérin, A. Hamwi and E. Flahaut, High energy density of primary lithium batteries working with sub-fluorinated few walled carbon nanotubes cathode, *J. Alloys Compd.*, 2017, **726**, 852-859.